

See discussions, stats, and author profiles for this publication at: <https://www.researchgate.net/publication/225046258>

Face-Centered-Cubic Large-Pore Periodic Mesoporous Organosilicas with Unsaturated and Aromatic Bridging Groups

ARTICLE *in* LANGMUIR · MAY 2012

Impact Factor: 4.46 · DOI: 10.1021/la301329c · Source: PubMed

CITATIONS

4

READS

49

4 AUTHORS, INCLUDING:



[Manik Mandal](#)

Lehigh University

22 PUBLICATIONS 207 CITATIONS

SEE PROFILE



[Amanpreet S Manchanda](#)

City University of New York - College of Staten ...

3 PUBLICATIONS 4 CITATIONS

SEE PROFILE



[Jianqin Zhuang](#)

City University of New York - College of Staten ...

25 PUBLICATIONS 499 CITATIONS

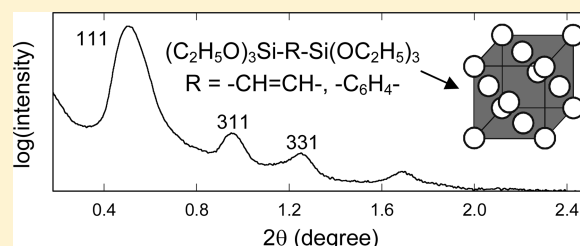
SEE PROFILE

Face-Centered-Cubic Large-Pore Periodic Mesoporous Organosilicas with Unsaturated and Aromatic Bridging Groups

Manik Mandal,^{†,§} Amanpreet S. Manchanda,^{†,‡} Jianqin Zhuang,[†] and Michal Kruk^{†,‡,*}[†]Department of Chemistry, College of Staten Island, City University of New York, 2800 Victory Boulevard, Staten Island, New York 10314, United States[‡]Graduate Center, City University of New York, 365 Fifth Avenue, New York, New York 10016, United States

Supporting Information

ABSTRACT: Large-pore ethenylene-bridged ($-\text{CH}=\text{CH}-$) and phenylene-bridged ($-\text{C}_6\text{H}_4-$) periodic mesoporous organosilicas (PMOs) with face-centered-cubic structure ($Fm3m$ symmetry) of spherical mesopores were synthesized at 7 °C at low acid concentration (0.1 M HCl) using Pluronic F127 triblock copolymer surfactant in the presence of aromatic swelling agents (1,3,5-trimethylbenzene, xylenes–isomer mixture, and toluene). In particular, this work reports an unprecedented block-copolymer-templated well-ordered ethenylene-bridged PMO with cubic structure of spherical mesopores and an unprecedented block-copolymer-templated face-centered cubic phenylene-bridged PMO, which also has an exceptionally large unit-cell size and pore diameter. The unit-cell parameters of 30 and 25 nm and the mesopore diameters of 14 and 11 nm (nominal BJH-KJS pore diameters of 12–13 and 9 nm) were obtained for ethenylene-bridged and phenylene-bridged PMOs, respectively. Under the considered reaction conditions, the unit-cell parameters and pore diameters were found to be similar when the three different methyl-substituted benzene swelling agents were employed, although the degree of structural ordering appeared to improve for phenylene-bridged PMOs in the sequence of decreased number of methyl groups on the benzene ring.



INTRODUCTION

The use of block copolymers as micellar templates^{1,2} for the synthesis of periodic mesoporous organosilicas (PMOs)^{3–6} brought new vast opportunities to the synthesis^{7–10} of these remarkably diverse and potentially practically important materials.^{11–18} While block-copolymer-templated PMOs with 2-dimensional hexagonal structures of cylindrical mesopores were extensively studied and successfully synthesized with a variety of framework compositions,^{7,19–25} the application of block-copolymer templates in the synthesis of PMOs with spherical mesopores arranged in well-defined cubic structures proved to be challenging. This was quite unexpected, because the use of alkylammonium surfactants readily afforded PMOs with spherical mesopores, including 3-D hexagonal,^{3,26} cubic $Pm3n$,^{26–30} and face-centered cubic $Fm3m$ structures.^{28,31,32} The first reported, and by far the most common, copolymer-templated PMOs with spherical mesopores were ethylene-bridged organosilicas (with $-\text{CH}_2\text{CH}_2-$ bridging groups).^{10,33–42} Even in this case, early work involved difficulty in the structure formation⁸ or the identification of an ordered structure type,¹⁰ which were resolved primarily through the use of inorganic salts in the synthesis,³³ although the use of the latter is not necessary for the formation of the material under certain conditions.^{34,39} The success in the synthesis of other compositions of block-copolymer-templated PMOs with spherical mesopores was quite limited. In the case of the first cubic phenylene-bridged PMO of this kind, no structure type

was assigned and the pore diameter was small.³⁰ Phenylene-bridged and thiophene-bridged PMOs with highly ordered body-centered cubic structures ($Im3m$ symmetry) were reported, but their pore diameter was also small (capillary condensation pressure of nitrogen below the relative pressure of 0.60).⁴³ Methylene-bridged PMO, presumably with face-centered cubic structure, was also reported, but its degree of ordering was low.⁴⁴ Notably, cubic ethenylene-bridged PMO with unsaturated bridging groups and spherical mesopores has not been reported, except for Pluronic P123-templated PMO, which contained a certain fraction of the face-centered cubic structure but was not a homogeneous, well-defined material.⁴⁵

Because of the importance of PMOs with aromatic^{6,17,30,46–49} and unsaturated bridging groups,^{4,5,17,50,51} which can be chemically modified and functionalized^{14,5,46,48} and which can induce the formation of crystal-like pore walls,^{17,43,46,52} improved syntheses of such materials with large spherical mesopores would be beneficial. To this end, herein block-copolymer-templated syntheses of face-centered cubic ethenylene-bridged and phenylene-bridged PMOs are reported. The PMOs were formed at subambient temperatures, which were known to afford ethylene-bridged PMOs with large mesopores (diameter up to 17 nm or even more)^{38–40} and

Received: August 15, 2011

Revised: May 19, 2012

Published: May 21, 2012

weakly ordered methylene-bridged PMO,⁴⁴ when Pluronic F127 (EO₁₀₆PO₇₀EO₁₀₆) was used as a surfactant. 1,3,5-Trimethylbenzene (TMB), which is well-known as a micelle expander in low-temperature synthesis,^{38,39,44,53–55} as well as xylenes (mixture of isomers) and toluene, which were recently shown by us to be superior micelle expanders under the subambient conditions,^{39,56} were employed. The formation of the well-ordered structure took place at an acid concentration of 0.1 M that was lower than that usually employed in the low-temperature syntheses.^{38,39,53,56} This acid concentration was recently shown by others to be suitable for the synthesis of ethylene-bridged PMOs with large unit-cell sizes.⁴⁰ Under the conditions outlined above, it was possible to obtain unprecedented well-ordered face-centered cubic ethenylene-bridged and phenylene-bridged PMOs with spherical mesopores of diameters above 10 nm, which are unusually large for such PMOs.

MATERIALS AND METHODS

Materials. In a typical synthesis of ethenylene-bridged PMO, 0.5 g of Pluronic F127 (EO₁₀₆PO₇₀EO₁₀₆) was placed in 30 g of 0.10 M aqueous HCl solution, which was followed by magnetic stirring until the whole polymer dissolved at 7 °C. Then 0.5 g toluene (or other swelling agent: xylenes, mixture of isomers that may contain ethylbenzene, or 1,3,5-trimethylbenzene) and 2.5 g of KCl was added. After 2 h, 1.73 mL of bis(triethoxysilyl)ethylene, (C₂H₅O)₃Si-CH=CH-Si(OC₂H₅)₃, was added. The reaction mixture was stirred for 1 d at 7 °C in a covered container. Then, the whole solution was treated hydrothermally at 100 °C for 1 d. The resulting as-synthesized material was then filtered, washed with deionized water, and dried at ~60 °C in a vacuum oven. Finally, the material was calcined at 350 °C under argon atmosphere for 5 h (heating ramp 2 °C/min). Alternatively, the samples were extracted using 5 mL of HCl in 60 mL of ethanol at 60 °C for 6 h.³⁸ After the first extraction, the sample was filtered out and the extraction was repeated.

In a typical synthesis of phenylene-bridged PMO, 0.5 g of Pluronic F127 was added to 30 g of 0.10 M HCl solution, which was followed by magnetic stirring until the whole polymer dissolved at 7 °C. Then 0.5 g of toluene (or xylenes or TMB) and 2.5 g of KCl was added. After 2 h, 1.86 mL of bis(triethoxysilyl)benzene (BTEB) was added. The reaction mixture was stirred for 1 d at 7 °C in a covered container. Then the whole solution was treated hydrothermally at 100 °C for 1 d. The resulting as-synthesized material was then filtered, washed with deionized water, and dried at ~60 °C in a vacuum oven. Finally, the material was calcined at 250 °C under air for 5 h (heating ramp 2 °C/min). The calcination conditions follow earlier work of others²⁰ and us⁵⁷ on 2-D hexagonal phenylene-bridged PMOs.

Measurements. Small-angle X-ray scattering (SAXS) patterns were recorded on Bruker Nanostar U instrument equipped with rotating anode Cu K α radiation source operated at 50 kV and 24 mA and with Vantec 2000 2-dimensional detector. Samples were placed in the hole of an aluminum sample holder and secured on both sides using a Kapton tape. Nitrogen adsorption was measured on Micromeritics ASAP 2020 volumetric adsorption analyzer at -196 °C. The samples were outgassed at 140 °C in the degass port of ASAP 2020 before the analysis. Transmission electron microscopy (TEM) images were recorded on FEI Tecnai Spirit microscope operated at an accelerating voltage of 120 kV and JEOL JEM-2000 microscope operated at an accelerating voltage of 200 kV. The samples were sonicated using an adequate amount of ethanol as a medium. After that, the dispersions containing the samples were drop-cast on carbon coated copper grids. The solvent was evaporated under air to dryness before TEM analysis. ²⁹Si magic angle spinning (MAS) and cross-polarization (CP) MAS NMR experiments were carried out on a Varian INOVA 300 wide bore spectrometer equipped with a superconducting magnet with a field of 7.1 T. The operating frequency for ²⁹Si measurements was 59.6 MHz. The samples were packed into a 5 mm zirconia rotor and loaded into a 5 mm Doty XC-5

CP/MAS probe and spun at 6–8 kHz. A total of 1000–3500 scans were acquired depending on the sensitivity of a given sample. The recycle delay was 3 s, the contact time was 1.0 ms, and the 90° pulse was 4.5 ms. The chemical shift reference was DSS. Weight change patterns were acquired under air using a TA Instruments Hi-Res 2950 thermogravimetric analyzer.

Calculations. The BET specific surface area (S_{BET}) was calculated from nitrogen adsorption isotherm in the relative pressure range from 0.04 to 0.20.⁵⁸ Total pore volume (V_t) was determined from the amount adsorbed at a relative pressure of 0.99.⁵⁸ The micropore volume (V_{mic}) was calculated using the α_s plot method in the standard reduced adsorption, α_s , range from 0.9 to 1.2 using LiChrospher Si-1000 as a reference adsorbent.^{39,59} The sum of the primary mesopore volume (V_p) and the micropore volume was evaluated in the α_s range from 2 to 2.5.³⁹ The mesopore volume was calculated by subtracting V_{mi} from $V_{\text{mi}} + V_p$ estimated as discussed above. Pore size distributions (PSDs) were determined from adsorption branches of the isotherms using the Barrett–Joyner–Halenda (BJH) method⁶⁰ with KJS correction for cylindrical mesopores⁶¹ and the statistical film thickness curve for a macroporous silica gel LiChrospher Si-1000.⁵⁹ This method is known to underestimate the diameter of spherical mesopores by ~2 nm in the considered pore size range.⁶² Therefore, the pore diameter was also evaluated for most samples using a geometrical relation proposed by Ravikovitch and Neimark for materials with face-centered cubic structures of spherical mesopores:⁶³

$$w_d = a \left(\frac{6}{\pi \nu} \frac{V_p \rho}{1 + V_p \rho + V_{\text{mi}} \rho} \right)^{1/3} \quad (1)$$

where a is the unit-cell parameter calculated from the position of (111) peak on the SAXS pattern, ν is the number of spherical mesopores in the unit cell (4 for fcc structure), and ρ is the framework density. In the case of the phenylene-bridged PMO, the framework density was estimated as 1.42 g cm⁻³ from the framework densities reported for disordered phenylene-bridged organosilicas.⁶⁴ For ethenylene-bridged PMOs, the framework density was assumed to be equal to that reported for ethylene-bridged organosilicas (an average of 1.52 g cm⁻³)⁶⁴ in lieu of the value for the ethenylene-bridged framework.

RESULTS AND DISCUSSION

Face-Centered Cubic Ethenylene-Bridged PMOs. As can be seen in Figure 1 and Figure S1, ethenylene-bridged PMOs synthesized in the presence of TMB, xylenes, and toluene exhibited very well-resolved SAXS patterns characteristic of the face-centered cubic structure ($Fm\bar{3}m$ symmetry; for peak indexing, see Table S1). The unit-cell parameters were

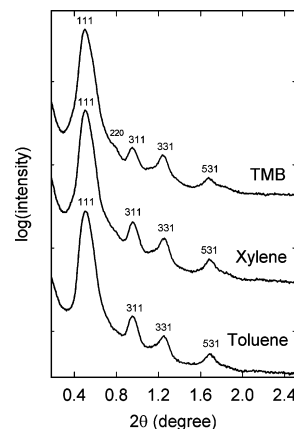


Figure 1. SAXS patterns of face-centered-cubic ethenylene-bridged PMOs synthesized using different swelling agents and extracted with ethanol/HCl mixture.

Table 1. Properties of Face-Centered Cubic PMOs with Ethenylene and Phenylene Bridging Groups Synthesized in the Presence of Different Swelling Agents^a

bridging group	swelling agent	<i>a</i> (nm)	<i>S</i> _{BET} (m ² /g)	<i>V</i> _t (cm ³ /g)	<i>V</i> _p (cm ³ /g)	<i>V</i> _{mic} (cm ³ /g)	<i>w</i> _{KJS} (nm)	<i>w</i> _d (nm)
ethenylene	toluene	30.4 (31.2)	235	0.20	(0.11) ^b	0.07	13.2	<i>c</i>
ethenylene	xylene	30.6 (31.2)	244	0.25	0.18	0.05	12.5	14.0
ethenylene	TMB	30.6 (31.5)	354	0.34	0.24	0.09	12.2	14.9
phenylene	toluene	25.3 (27.6)	426	0.32	0.15	0.12	9.4	10.6
phenylene	xylene	25.3 (27.1)	520	0.36	0.19	0.16	9.4	11.2
phenylene	TMB	25.3 (27.3)	413 ^b	0.25 ^b	(0.08) ^b	0.16 ^b	9.0	<i>c</i>

^aNotation: *a*, unit-cell parameter for extracted ethenylene-bridged or calcined phenylene-bridged sample calculated from (111) interplanar spacing (unit-cell parameter for as-synthesized sample is provided in parentheses); *S*_{BET}, BET specific surface area; *V*_t, total pore volume; *V*_p, primary mesopore volume; *V*_{mic}, micropore volume; *w*_{KJS}, pore diameter calculated using BJH-KJS method for cylindrical mesopores. *w*_d, pore diameter calculated using eq 1. ^bNot fully reliable because of apparently slow diffusion during the adsorption measurement or to incomplete extraction. ^cNot estimated because *V*_p was not available with acceptable accuracy.

essentially the same (30.4–30.6 nm for extracted samples and 27.8 nm for calcined samples; see Table 1 and Table S2) and the SAXS patterns were similar, although their resolution for the calcined samples improved slightly (see Figure S1) as the swelling agent was changed from TMB to xylenes and toluene. The unit-cell parameters for as-synthesized samples were also similar for the three samples (31.2–31.5 nm). TEM images for ethenylene-bridged PMO prepared in the presence of xylene (see Figure 2 and Figure S2) revealed highly ordered structures

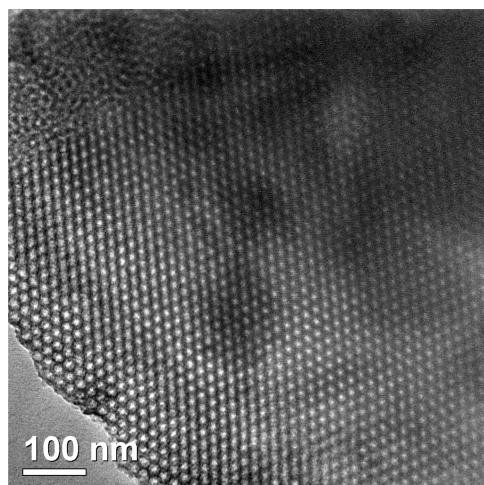


Figure 2. Transmission electron microscopy image of calcined ethenylene-bridged PMOs (synthesized using xylene as a swelling agent) that can be identified as [110] projection of face-centered-cubic structure. An apparently disordered domain is seen in top left corner.

with large ordered domain sizes but also some apparently weakly ordered or disordered regions on the edges of some particles. Domains that can be identified as [110] projection of face-centered cubic structure are seen (see for instance Figure 2). In addition, TEM image shown in Figure S2 shows a very large ordered domain that can be identified as the [110] projection of the face-centered cubic structure with stacking faults that correspond to 3-dimensional hexagonal packing sequence, as reported earlier for FDU-1 silica.⁶² The presence of apparently disordered regions (see for instance upper part of Figure 2) is not immediately inferable from the SAXS patterns, so they are likely to constitute a minor part of the sample. TEM image of PMO prepared in the presence of TMB (Figure S3) indicates the presence of ordered and apparently disordered domains coexisting one next to another. However, for these

PMOs, significant parts of particles were too dark (apparently too thick) to be well visible in TEM, and TEM with higher acceleration voltage showed the highly ordered structures more readily, which suggests that many of the dark regions may correspond to well-ordered domains. This contention is consistent with very intense and well-resolved SAXS patterns. The considered materials are first examples of block-copolymer-templated ethenylene-bridged PMOs with highly ordered *Fm3m* structure, as seen from SAXS, although they may still contain a certain, presumably small, fraction of weakly ordered or disordered domains. Previously, the use of a different block copolymer (Pluronic P123, EO₂₀PO₇₀EO₂₀) afforded an ethenylene-bridged PMO containing some face-centered cubic domains, but this PMO was found to be a phase mixture⁴⁵ and its SAXS pattern was not indexable. The unit-cell parameters observed for PMOs considered here were larger than those typically observed for PMOs with spherical mesopores,^{33,43} although some ethylene-bridged PMOs with *Fm3m* symmetry had larger unit-cell sizes.^{38,39}

Initially, the surfactant from ethenylene-bridged PMOs was removed by calcination under argon at 350 °C. While the materials remained highly ordered and had good pore accessibility and narrow pore size distributions (see Figures S1, S4, and S5), ²⁹Si NMR (Figure S6) showed that a substantial fraction of Si–C bonds was cleaved, because T sites (peaks at –67 and ~–80 ppm) were accompanied by a substantial fraction of Q sites (at –100 to –120 ppm). Possibly, most of the bridging ethenylene groups converted to pendent vinyl groups through the transformation described for ethenylene-bridged 2-D hexagonal PMOs⁶⁵ and similar in nature to what was originally reported for methylene-bridged PMOs.^{66,67} Therefore, an extraction with ethanol and HCl was carried out,³⁸ and the resulting PMOs exhibited T sites at –76 and –83 ppm, whereas there was no signal related to Q sites and thus no evidence of cleavage of Si–C bonds (see ²⁹Si MAS NMR spectrum in Figure S7). Some surfactant (~16 wt %, as estimated by TGA) still remained in the materials after extraction, but the mesopores were accessible (in most cases, see below).

Shown in Figure 3 and Figure S4 are nitrogen adsorption isotherms for the extracted and calcined ethenylene-bridged PMOs. The extracted and calcined samples exhibited steep capillary condensation steps at relative pressures of ~0.82 and ~0.79, respectively, and nearly vertical capillary evaporation steps at ~0.48–0.49, which happened to be a lower limit of adsorption–desorption hysteresis.⁶⁸ The adsorption isotherms were characteristic of materials with uniform, large mesopores

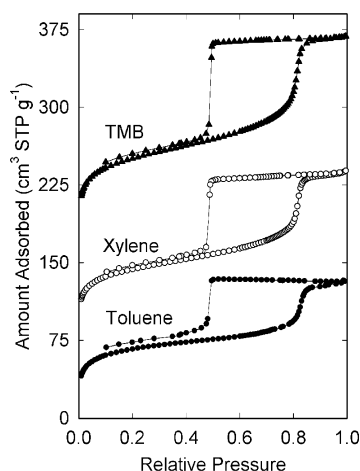


Figure 3. Nitrogen adsorption isotherms for extracted face-centered-cubic ethynylene-bridged PMOs synthesized using different swelling agents. Isotherms for samples prepared with xylene and TMB were offset vertically by 75 and 150 $\text{cm}^3 \text{STP g}^{-1}$, respectively.

accessible through constrictions of diameter below 5 nm (based on the position of the capillary evaporation step).^{68,69} The calcined PMOs exhibited specific surface areas of $\sim 430 \text{ m}^2 \text{g}^{-1}$, total pore volumes of $0.35 \text{ cm}^3 \text{g}^{-1}$, primary mesopore volumes of $\sim 0.21 \text{ cm}^3 \text{g}^{-1}$, and micropore volume of $\sim 0.12 \text{ cm}^3 \text{g}^{-1}$ (see Table S2). The extracted sample prepared in the presence of TMB exhibited similar total pore volume and primary mesopore volume (see Table 1), whereas its micropore volume and specific surface area were somewhat lower. The extracted PMOs prepared in the presence of xylene and toluene showed lower mesopore volumes and total pore volumes, especially in the case of the sample prepared with toluene. Apparently, the efficiency of the extraction to remove the surfactant and/or to make the mesopores accessible decreased as the swelling agent changed from TMB to xylene and toluene. Anyway, it is clear that the primary mesopore volumes for most of these PMOs were higher than those reported in our previous study of ethynylene-bridged PMOs with saturated bridging groups.³⁹ Pore size distributions derived from the adsorption isotherms (Figure 4 and Figure S5) were very narrow and centered at

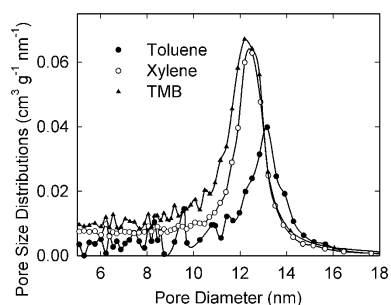


Figure 4. Pore size distributions of face-centered-cubic ethynylene-bridged PMOs synthesized using different swelling agents.

$\sim 12\text{--}13 \text{ nm}$ and $\sim 11 \text{ nm}$ for extracted and calcined samples, respectively (Table 1 and Table S2). More reliable estimates of the pore diameter through eq 1 afforded values of $\sim 13\text{--}15 \text{ nm}$ (see Table 1 and Table S2). The pore diameters observed for our ethynylene-bridged PMOs with spherical mesopores were larger than pore diameters of most well-ordered PMOs with spherical mesopores reported previously. Only ethylene-

bridged PMOs exhibited larger pore diameters if they were synthesized under appropriate conditions.^{38–40}

Face-Centered Cubic Phenylene-Bridged PMOs. SAXS patterns of phenylene-bridged PMOs synthesized under the considered conditions (Figure 5) can also be identified as those

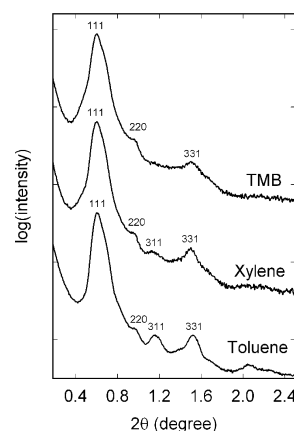


Figure 5. SAXS patterns for face-centered-cubic phenylene-bridged PMOs synthesized using different swelling agents and calcined at 250°C under air.

characteristic of well-ordered face-centered cubic structure. Clear shoulders on the right side of (111) peaks are likely to correspond to (200) reflections,⁷⁰ which was rarely seen on SAXS patterns of materials with *Fm3m* symmetry.^{39,53,54,56,71} Our PMOs appear to be the first block-copolymer-templated phenylene-bridged PMOs with *Fm3m* symmetry. The resolution of SAXS patterns for the phenylene-bridged PMOs improved as TMB was replaced with xylenes and toluene. The unit-cell parameter for calcined samples was 25.3 nm and was insensitive to the change in the swelling agent used, whereas as-synthesized samples exhibited the unit-cell parameter $27.1\text{--}27.6 \text{ nm}$, which was also very similar for all three samples (see Table 1). TEM of selected samples showed many ordered domains, although some of them were small in size (Figures S8 and S9), being too small to allow for their identification. Significant parts of the samples were too thick to give clear TEM images, so the structural identification by TEM was not achieved. Some parts of the edges of the particles appeared to be weakly ordered or disordered, and apparently non-mesoporous content was seen in some places, either as an envelope around the edge of the particles or as separate domains. Although the unit-cell parameter for the phenylene-bridged cubic PMOs was smaller than that for their ethynylene-bridged counterparts, it was still much larger than the unit-cell parameter of $\sim 15 \text{ nm}$ reported for body-centered cubic phenylene-bridged PMOs.⁴³ The other reported cubic phenylene-bridged PMO, whose structure was not assigned, also appeared to exhibit a smaller unit-cell parameter, based on the position of its main X-ray diffraction peak at 0.8° .³⁰ It is notable that the cubic phenylene-bridged PMOs with spherical mesopores reported earlier^{30,43} were synthesized at quite low acid concentrations ($0.05\text{--}0.07 \text{ M HCl}$ or $0.05 \text{ M H}_2\text{SO}_4$), which is similar to the acid concentration used in our synthesis (0.1 M HCl).

Shown in Figure 6 are nitrogen adsorption isotherms for the phenylene-bridged PMOs. They were quite similar to those discussed earlier for PMOs with unsaturated bridging groups, but the capillary condensation pressure was somewhat lower.

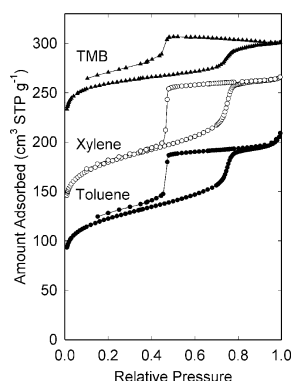


Figure 6. Nitrogen adsorption isotherms of face-centered-cubic phenylene-bridged PMOs synthesized using different swelling agents. Isotherms for samples prepared in the presence of xylene and TMB were offset vertically by 30 and 140 cm³ STP g⁻¹, respectively.

More importantly, the low-pressure adsorption–desorption hysteresis (below relative pressure of ~ 0.40) was observed for PMO prepared in the presence of TMB. The use of different calcination temperatures and/or atmospheres (nitrogen or argon instead of air) afforded materials with similar adsorption properties. This indicates that the size of entrances to the mesopores in the structure of this PMO was close to the size of the nitrogen molecule used in adsorption measurements, and the low-pressure hysteresis was due to slow diffusion of nitrogen into the mesopores of the considered PMO. Low-pressure hysteresis, although much less pronounced, might have occurred also for the phenylene-bridged PMO synthesized in the presence of toluene. The specific surface areas of the PMOs were 410–520 m² g⁻¹, total pore volumes were 0.25–0.32 cm³ g⁻¹, primary mesopore volumes were 0.15–0.19 cm³ g⁻¹ (the value of 0.08 cm³ g⁻¹ for PMO prepared in the presence of TMB is likely to be significantly underestimated because of the aforementioned diffusion problem), and the micropore volumes were 0.12–0.16 cm³ g⁻¹. The pore size distributions (Figure 7) were narrow and were centered at 9.0–

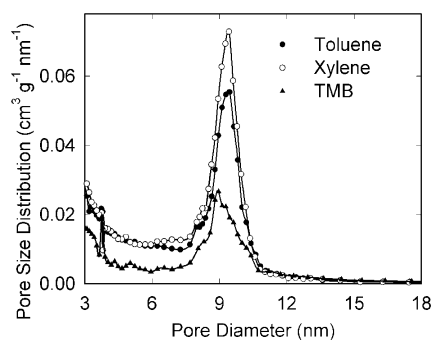


Figure 7. Pore size distributions of face-centered-cubic phenylene-bridged PMOs synthesized using different swelling agents.

9.4 nm (see Table 1), and pore diameters calculated using eq 1 were ~ 11 nm. The pore sizes of our cubic phenylene-bridged PMOs were much larger than those of their literature counterparts^{30,43} (as clearly seen from the capillary condensation relative pressure of ca. 0.45–0.55 for those PMOs vs 0.75 for our PMOs), which can be attributed to our successful use of swelling agents. It should be noted that swelling agents were used before to promote the formation of spherical single-micelle-templated phenylene-bridged organosilica particles

using Pluronic F127 surfactant,^{42,72} but the extension of this synthesis on well-defined PMO was not successful.⁴²

²⁹Si NMR showed that while the calcination at 250 °C under air preserves a majority of T sites (at -71 and -80 ppm), but Q sites were also seen at -100 to -110 ppm, and thus a small fraction of Si–C bonds in the bridging phenylene moieties was cleaved during the calcination (see Figure S10). The calcination at 325 °C under nitrogen and at 350 °C under argon led to a comparable (perhaps slightly larger) extent of cleavage. However, as seen for ethylene-bridged PMOs discussed above, the extraction is a viable procedure for the surfactant removal while avoiding the degradation of the bridging groups.

Influence of Synthesis Mixture Composition on Organosilica Structure. Additional experiments were performed to understand the influence of the synthesis mixture composition on the structure of phenylene-bridged organosilica materials prepared at 7 °C in 0.10 M HCl solution. In the absence of a swelling agent, a material was obtained whose SAXS pattern featured one broad peak (see Figure S11), showing that a well-ordered structure did not form. The peak was located at higher angles in comparison to the position of the main peak on SAXS patterns of the phenylene-bridged PMOs (Figure 5), indicating smaller repeating distances in the structure, as expected in the case where the templating micelles were not swollen. Similar results were reported earlier for ethylene-bridged organosilicas.³⁹

The influence of the ratio of the organosilica precursor to the surfactant was investigated to verify if it is possible to obtain single-micelle-templated nanoparticles at low precursor/surfactant ratios, as demonstrated recently in the case of more highly acidic conditions (2 M HCl), where individual particles can readily be obtained.⁴² The syntheses were performed with BTEB and xylene as a swelling agent, the latter being used in double relative amount in comparison to the synthesis conditions described above. The structural parameters derived from SAXS and nitrogen adsorption for the resulting samples are listed in Table S3. The organosilica prepared with the volume of BTEB used for the samples described above (1.86 mL per 0.5 g of F127) exhibited a well ordered face-centered cubic structure (see Figure 8) with uniform mesopores, as seen from nitrogen adsorption (see Figures 9 and 10). The increase in the relative amount of the swelling agent brought an increase in the nominal pore diameter by about 2 nm (from $w_{\text{KJS}} = 9.4$

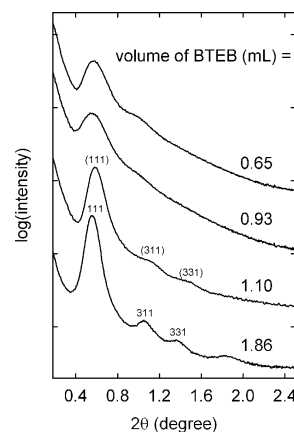


Figure 8. SAXS patterns for phenylene-bridged organosilicas synthesized using different organosilica precursor/surfactant ratios in the presence of xylene.

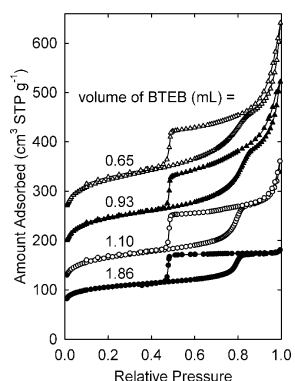


Figure 9. Nitrogen adsorption isotherms for phenylene-bridged organosilicas synthesized using different organosilica precursor/surfactant ratios in the presence of xylene. Isotherms for samples prepared with 1.10, 0.93, and 0.65 mL of BTEB were offset vertically by 50, 120, and 190 $\text{cm}^3 \text{STP g}^{-1}$, respectively.

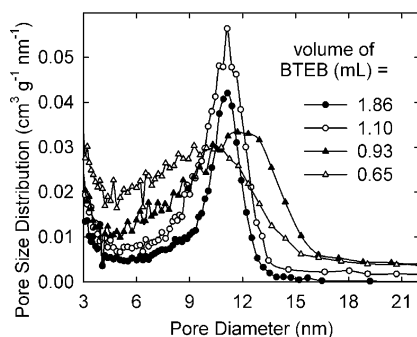


Figure 10. Pore size distributions for phenylene-bridged organosilicas synthesized using different organosilica precursor/surfactant ratios in the presence of xylene.

to 11.1 nm, see Table 1 and Table S3), so the pore diameter of the considered PMOs can be tailored by adjusting the amount of the swelling agent. The lowering of the volume of BTEB to 1.10 mL (59% of the originally used volume) afforded an organosilica with a less well resolved SAXS pattern with peak/shoulder positions similar to those for PMO prepared with 1.86 mL BTEB (Figure 8). TEM (Figure S12) revealed that the organosilica prepared with 1.10 mL of BTEB consisted of small particles with fairly uniform pores that were ordered in many areas. The particles were significantly agglomerated and there was no evidence for the formation of single-micelle-templated particles (that is, hollow spheres in this case). The sample exhibited an appreciable uptake of nitrogen at pressure above the capillary condensation pressure in the uniform mesopores (above $0.80 p/p_0$), which indicates the presence of secondary mesopores, which can be identified as interparticle pores on the basis of TEM (Figure S12). The pore size distribution was still narrow and the pore diameter was essentially the same as that for the sample synthesized using higher relative amount of BTEB (Figure 10).

A similar secondary porosity was inferred from the isotherms of the samples prepared with even lower relative amounts of BTEB (0.93 and 0.65 mL per 0.5 g of Pluronic F127; Figure 9). However, in these cases, the pore size distributions were significantly broader (Figure 10) and SAXS patterns became poorly resolved (with one peak and one weak shoulder). TEM (see for instance Figure S13) indicated no clear structural ordering within small and typically heavily agglomerated

particles. The particles featured multiple mesopores and there was no clear evidence of the formation of single-micelle-templated nanoparticles. This result is somewhat surprising, because under more strongly acidic conditions (2 M HCl), individual hollow spherical particles and their loose aggregates were seen for 0.93 mL of BTEB (per 0.5 g of Pluronic F127).⁴² Clearly, 0.1 M HCl solution environment favors the formation of particles with multiple pores, and thus templated by multiple micelles (perhaps micellar aggregates) instead of single-micelle-templated particles. It was postulated that in the Pluronic-templated synthesis of silicas under acidic conditions poly(ethylene oxide) (PEO) chains are associated with hydronium ions.² It was hypothesized that in single-micelle-templated synthesis of spherical particles using Pluronic surfactants, outer parts of PEO blocks of the triblock copolymer surfactant molecules provide the stabilization, thus preventing aggregation and cross-linking⁷³ of the hybrid surfactant-silica micelles.⁷⁴ It is suggested herein that the association of these parts of PEO blocks with hydronium ions may lead to the additional stabilization of individual hybrid surfactant-silica micelles. However, at reduced acidity, this stabilization may be insufficient, and multimicelle-templated particles are obtained. Perhaps micelle aggregates are present in the solution already before the addition of the framework precursor and do not break down into individual hybrid surfactant-silica micelles at any stage of the process. Alternatively, in weakly acidic conditions, the organosilica precursor may hydrolyze and condense primarily in the outer part of the coronas of the micelles, especially for low precursor/surfactant ratios, and cross-linking between the hybrid surfactant-silica micelles is inevitable. The fact that the volumes of the uniform (primary) mesopores of PMOs formed in 0.1 M HCl (as reported herein) tend to be higher than those for their counterparts³⁹ prepared in 2 M HCl is consistent with the organosilica precursor condensation further away from the centers of the templating micelles in the present case.

The PMOs discussed herein and many Pluronic-F127-templated ethylene-bridged PMOs obtained using swelling agents (TMB, xylene, or toluene)^{38,39} exhibit a face-centered cubic structure, whereas Pluronic-F127-templated PMOs with spherical mesopores synthesized in the absence of a swelling agent tend to exhibit a body-centered cubic structure.^{33,37,43} It was shown that, in the case of poly(ethylene oxide)–poly(butylene oxide) surfactants with similar size of the poly(butylene oxide) block, the increase in size of the PEO block favors the formation of body-centered cubic structure over the face-centered cubic structure.⁷⁵ The proposed explanation was that the micelles of surfactants with shorter PEO blocks behaved like hard spheres and formed a closed-packed structure, whereas the micelles of surfactants with longer PEO blocks behaved like soft spheres and packed in body-centered cubic structures.⁷⁵ It is hypothesized herein that when the swelling agent is present (as in the present study), the swollen micelles of Pluronic F127 (or composite silica/F127 micelles) tend to behave like hard spheres and pack in the face-centered cubic structure, while in the absence of the swelling agent, the micelles (or composite micelles) tend to behave like soft spheres, which may pack in body-centered cubic arrays.

In the present study, TMB, xylene, and toluene were employed as swelling agents, because they were demonstrated to be suitable micelle expanders for Pluronic-F127-templated PMO synthesis.^{38,39} Moreover, many other swelling agent candidates, such as linear hydrocarbons or alkylbenzenes with

larger number of carbon atoms in alkyl substituents on the benzene ring (e.g., triethylbenzene), are likely to be taken up to a lower extent by Pluronic F127 micelles^{39,56} and thus are expected to be inferior swelling agents.³⁹ Although benzene can be used as a swelling agent for PMOs³⁹ and silicas⁷⁶ with spherical mesopores, it is more difficult to optimize conditions in which it renders well-defined large-pore materials,³⁹ and thus it was not used in the present study.

CONCLUSIONS

The lowering of the acid concentration from the typically used 2 to 0.1 M combined with the low initial temperature of 7 °C allowed us to synthesize two unique types of well-defined PMOs: face-centered cubic organosilicas with ethynylene and phenylene bridging groups in the framework. The PMOs with unsaturated bridging groups were very well ordered and exhibited large pore diameters of ~14 nm. The PMOs with aromatic bridging groups were also well-ordered and exhibited ~11 nm mesopores, which were large in comparison to those of their close counterparts reported earlier. Although the pore diameter was largely independent of the swelling agent used, the degree of structural ordering improved for phenylene-bridged PMOs in the sequence: TMB < xylenes < toluene, being the best for the latter. In some cases of phenylene-bridged PMOs, low-pressure hysteresis was observed, indicating that the passages to the mesopores were of diameter comparable to the size of nitrogen molecule. The conditions involving low initial synthesis temperature and low acid concentration are likely to provide a convenient avenue for the synthesis of PMOs of other framework compositions.

ASSOCIATED CONTENT

Supporting Information

Tables with relative peak positions and with structural parameters derived from nitrogen adsorption and SAXS. Figures with SAXS patterns, adsorption isotherms, and pore size distributions. TEM images and NMR spectra. This material is available free of charge via the Internet at <http://pubs.acs.org>.

AUTHOR INFORMATION

Corresponding Author

*E-mail: michal.kruk@csi.cuny.edu.

Present Address

[§]Department of Chemistry, Lehigh University, Bethlehem, Pennsylvania 18015, United States.

Notes

The authors declare no competing financial interest.

ACKNOWLEDGMENTS

NSF is gratefully acknowledged for support of this research (award DMR-0907487) and for funding the acquisition of SAXS/WAXS system through award CHE-0723028. Acknowledgment is made to the Donors of the American Chemical Society Petroleum Research Fund for partial support of this research (Award PRF No. 49093-DNIS). Professor Ruth Stark, Dr. Hsin Wang, and Dr. Subhasish Chatterjee (City College of New York) are gratefully acknowledged for help in preliminary NMR measurements. Dr. Liang Huang (CSI; currently ATRP Solutions, Pittsburgh, PA) is acknowledged for help in acquiring TEM images at CSI. The Imaging Facility at CSI is acknowledged for providing access to TEM. BASF is acknowledged for the donation of the F127 block copolymer.

REFERENCES

- (1) Zhao, D.; Feng, J.; Huo, Q.; Melosh, N.; Frederickson, G. H.; Chmelka, B. F.; Stucky, G. D. Triblock copolymer syntheses of mesoporous silica with periodic 50 to 300 angstrom pores. *Science* **1998**, *279*, 548–552.
- (2) Zhao, D.; Huo, Q.; Feng, J.; Chmelka, B. F.; Stucky, G. D. Nonionic Triblock and Star Diblock Copolymer and Oligomeric Surfactant Syntheses of Highly Ordered, Hydrothermally Stable, Mesoporous Silica Structures. *J. Am. Chem. Soc.* **1998**, *120*, 6024–6036.
- (3) Inagaki, S.; Guan, S.; Fukushima, Y.; Ohsuna, T.; Terasaki, O. Novel Mesoporous Materials with a Uniform Distribution of Organic Groups and Inorganic Oxide in Their Frameworks. *J. Am. Chem. Soc.* **1999**, *121*, 9611–9614.
- (4) Melde, B. J.; Holland, B. T.; Blanford, C. F.; Stein, A. Mesoporous Sieves with Unified Hybrid Inorganic/Organic Frameworks. *Chem. Mater.* **1999**, *11*, 3302–3308.
- (5) Asefa, T.; MacLachlan, M. J.; Coombs, N.; Ozin, G. A. Periodic mesoporous organosilicas with organic groups inside the channel walls. *Nature* **1999**, *402*, 867–871.
- (6) Yoshina-Ishii, C.; Asefa, T.; Coombs, N.; MacLachlan, M. J.; Ozin, G. A. Periodic mesoporous organosilicas, PMOs: fusion of organic and inorganic chemistry 'inside' the channel walls of hexagonal mesoporous silica. *Chem. Commun.* **1999**, 2539–2540.
- (7) Zhu, H.; Jones, D. J.; Zajac, J.; Roziere, J.; Dutartre, R. Periodic large mesoporous organosilicas from lyotropic liquid crystal polymer templates. *Chem. Commun.* **2001**, 2568–2569.
- (8) Cho, E.-B.; Kwon, K.-W.; Char, K. Mesoporous Organosilicas Prepared with PEO-Containing Triblock Copolymers with Different Hydrophobic Moieties. *Chem. Mater.* **2001**, *13*, 3837–3839.
- (9) Muth, O.; Schellbach, C.; Froeba, M. Triblock copolymer assisted synthesis of periodic mesoporous organosilicas (PMOs) with large pores. *Chem. Commun.* **2001**, 2032–2033.
- (10) Matos, J. R.; Kruk, M.; Mercuri, L. P.; Jaroniec, M.; Asefa, T.; Coombs, N.; Ozin, G. A.; Kamiyama, T.; Terasaki, O. Periodic Mesoporous Organosilica with Large Cagelike Pores. *Chem. Mater.* **2002**, *14*, 1903–1905.
- (11) Asefa, T.; Yoshina-Ishii, C.; MacLachlan, M. J.; Ozin, G. A. New nanocomposites: putting organic function "inside" the channel walls of periodic mesoporous silica. *J. Mater. Chem.* **2000**, *10*, 1751–1755.
- (12) MacLachlan, M. J.; Asefa, T.; Ozin, G. A. Writing on the wall with a new synthetic quill. *Chem.—Eur. J.* **2000**, *6*, 2507–2511.
- (13) Hatton, B.; Landskron, K.; Whitnall, W.; Perovic, D.; Ozin, G. A. Past, Present, and Future of Periodic Mesoporous Organosilicas The PMOs. *Acc. Chem. Res.* **2005**, *38*, 305–312.
- (14) Hunks, W. J.; Ozin, G. A. Challenges and advances in the chemistry of periodic mesoporous organosilicas (PMOs). *J. Mater. Chem.* **2005**, *15*, 3716–3724.
- (15) Stein, A.; Melde, B. J.; Schroden, R. C. Hybrid inorganic-organic meso-porous silicates-nanoscale reactors coming of age. *Adv. Mater.* **2000**, *12*, 1403–1419.
- (16) Hoffmann, F.; Cornelius, M.; Morell, J.; Froeba, M. Silica-based mesoporous organic-inorganic hybrid materials. *Angew. Chem., Int. Ed.* **2006**, *45*, 3216–3251.
- (17) Fujita, S.; Inagaki, S. Self-Organization of Organosilica Solids with Molecular-Scale and Mesoscale Periodicities. *Chem. Mater.* **2008**, *20*, 891–908.
- (18) Sayari, A.; Hamoudi, S. Periodic Mesoporous Silica-Based Organic-Inorganic Nanocomposite Materials. *Chem. Mater.* **2001**, *13*, 3151–3168.
- (19) Guo, W.; Park, J.-Y.; Oh, M.-O.; Jeong, H.-W.; Cho, W.-J.; Kim, I.; Ha, C.-S. Triblock Copolymer Synthesis of Highly Ordered Large-Pore Periodic Mesoporous Organosilicas with the Aid of Inorganic Salts. *Chem. Mater.* **2003**, *15*, 2295–2298.
- (20) Goto, Y.; Inagaki, S. Synthesis of large-pore phenylene-bridged mesoporous organosilica using triblock copolymer surfactant. *Chem. Commun.* **2002**, 2410–2411.
- (21) Vercaemst, C.; Ide, M.; Allaert, B.; Ledoux, N.; Verpoort, F.; Van Der Voort, P. Ultra-fast hydrothermal synthesis of diastereose-

lective pure ethenylene-bridged periodic mesoporous organosilicas. *Chem. Commun.* **2007**, 2261–2263.

(22) Bao, X. Y.; Li, X.; Zhao, X. S. Synthesis of Large-Pore Methylene-Bridged Periodic Mesoporous Organosilicas and Its Implications. *J. Phys. Chem. B* **2006**, *110*, 2656–2661.

(23) Morell, J.; Guengerich, M.; Wolter, G.; Jiao, J.; Hunger, M.; Klar, P. J.; Froeba, M. Synthesis and characterization of highly ordered bifunctional aromatic periodic mesoporous organosilicas with different pore sizes. *J. Mater. Chem.* **2006**, *16*, 2809–2818.

(24) Landskron, K.; Hatton, B. D.; Perovic, D. D.; Ozin, G. A. Periodic Mesoporous Organosilicas Containing Interconnected [Si(CH₃)₂]₃ Rings. *Science* **2003**, *302*, 266–269.

(25) Wang, W.; Xie, S.; Zhou, W.; Sayari, A. Synthesis of Periodic Mesoporous Ethylenesilica under Acidic Conditions. *Chem. Mater.* **2004**, *16*, 1756–1762.

(26) Lee, H. I.; Pak, C.; Yi, S. H.; Shon, J. K.; Kim, S. S.; So, B. G.; Chang, H.; Yie, J. E.; Kwon, Y.-U.; Kim, J. M. Systematic phase control of periodic mesoporous organosilicas using Gemini surfactants. *J. Mater. Chem.* **2005**, *15*, 4711–4717.

(27) Guan, S.; Inagaki, S.; Ohsuna, T.; Terasaki, O. Cubic Hybrid Organic-Inorganic Mesoporous Crystal with a Decaohedral Shape. *J. Am. Chem. Soc.* **2000**, *122*, 5660–5661.

(28) Liang, Y.; Erichsen, E. S.; Hanzlik, M.; Anwender, R. Facile Mesophase Control of Periodic Mesoporous Organosilicas under Basic Conditions. *Chem. Mater.* **2008**, *20*, 1451–1458.

(29) Sayari, A.; Hamoudi, S.; Yang, Y.; Moudrakovski, I. L.; Ripmeester, J. R. New Insights into the Synthesis, Morphology, and Growth of Periodic Mesoporous Organosilicas. *Chem. Mater.* **2000**, *12*, 3857–3863.

(30) Goto, Y.; Inagaki, S. Mesoporous phenylene-silica hybrid materials with 3D-cage pore structures. *Microporous Mesoporous Mater.* **2006**, *89*, 103–108.

(31) Liang, Y.; Hanzlik, M.; Anwender, R. PMO[KIT-5]-n: synthesis of highly ordered three-dimensional periodic mesoporous organosilicas with Fm3m symmetry. *Chem. Commun.* **2005**, 525–527.

(32) Liang, Y.; Hanzlik, M.; Anwender, R. Ethylene-bridged periodic mesoporous organosilicas with Fm3m symmetry. *J. Mater. Chem.* **2005**, *15*, 3919–3928.

(33) Guo, W.; Kim, I.; Ha, C.-S. Highly ordered three-dimensional large-pore periodic mesoporous organosilica with Im3m symmetry. *Chem. Commun.* **2003**, 2692–2693.

(34) Zhang, Z.; Tian, B.; Yan, X.; Shen, S.; Liu, X.; Chen, D.; Zhu, G.; Zhao, D.; Qiu, S. An easy route for the synthesis of ordered three-dimensional large-pore mesoporous organosilicas with Im-3m symmetry. *Chem. Lett.* **2004**, *33*, 1132–1133.

(35) Zhao, L.; Zhu, G.; Zhang, D.; Di, Y.; Chen, Y.; Terasaki, O.; Qiu, S. Synthesis and Structural Identification of a Highly Ordered Mesoporous Organosilica with Large Cage-like Pores. *J. Phys. Chem. B* **2005**, *109*, 764–768.

(36) Pauletti, A.; Handjani, S.; Fernandez-Martin, C.; Garvais, C.; Babonneau, F. A new example of periodic mesoporous SiCO glasses with cubic symmetry stable at 1000 °C. *J. Ceram. Soc. Jpn.* **2008**, *116*, 449–453.

(37) Guo, W.; Li, X.; Zhao, X. S. Understanding the hydrothermal stability of large-pore periodic mesoporous organosilicas and pure silicas. *Microporous Mesoporous Mater.* **2006**, *93*, 285–293.

(38) Zhou, X.; Qiao, S.; Hao, N.; Wang, X.; Yu, C.; Wang, L.; Zhao, D.; Lu, G. Q. Synthesis of Ordered Cubic Periodic Mesoporous Organosilicas with Ultra-Large Pores. *Chem. Mater.* **2007**, *19*, 1870–1876.

(39) Mandal, M.; Kruk, M. Large-Pore Ethylene-Bridged Periodic Mesoporous Organosilicas with Face-Centered Cubic Structure. *J. Phys. Chem. C* **2010**, *114*, 20091–20099.

(40) Hu, Y.; Qian, K.; Yuan, P.; Wang, Y.; Yu, C. Synthesis of large-pore periodic mesoporous organosilica. *Mater. Lett.* **2011**, *65*, 21–23.

(41) Na, W.; Wei, Q.; Zou, Z.-C.; Li, Q.-Y.; Nie, Z.-R. Mesoporous organosilicas with ultra-large pores: Mesophase transformation and bioadsorption properties. *J. Colloid Interface Sci.* **2010**, *346*, 61–65.

(42) Mandal, M.; Kruk, M. Family of Single-Micelle-Templated Organosilica Hollow Nanospheres and Nanotubes Synthesized through Adjustment of Organosilica/Surfactant Ratio. *Chem. Mater.* **2012**, *24*, 123–132.

(43) Cho, E.-B.; Kim, D.; Gorka, J.; Jaroniec, M. Three-dimensional cubic (Im3m) periodic mesoporous organosilicas with benzene- and thiophene-bridging groups. *J. Mater. Chem.* **2009**, *19*, 2076–2081.

(44) Kruk, M.; Hui, C. M. Thermally Induced Transition between Open and Closed Spherical Pores in Ordered Mesoporous Silicas. *J. Am. Chem. Soc.* **2008**, *130*, 1528–1529.

(45) Vercaemst, C.; de Jongh, P. E.; Meeldijk, J. D.; Goderis, B.; Verpoort, F.; Van Der Voort, P. Ethenylene-bridged periodic mesoporous organosilicas with ultra-large mesopores. *Chem. Commun.* **2009**, 4052–4054.

(46) Inagaki, S.; Guan, S.; Ohsuna, T.; Terasaki, O. An ordered mesoporous organosilica hybrid material with a crystal-like wall structure. *Nature* **2002**, *416*, 304–307.

(47) Kapoor, M. P.; Inagaki, S.; Ikeda, S.; Kakiuchi, K.; Suda, M.; Shimada, T. An Alternate Route for the Synthesis of Hybrid Mesoporous Organosilica with Crystal-Like Pore Walls from Allylorganosilane Precursors. *J. Am. Chem. Soc.* **2005**, *127*, 8174–8178.

(48) Kapoor, M. P.; Kasama, Y.; Yanagi, M.; Yokoyama, T.; Inagaki, S.; Shimada, T.; Nanbu, H.; Juneja, L. R. Cubic phenylene bridged mesoporous hybrids from allylorganosilane precursors and their applications in Friedel-Crafts acylation reaction. *Microporous Mesoporous Mater.* **2007**, *101*, 231–239.

(49) Kuroki, M.; Asefa, T.; Whitnall, W.; Kruk, M.; Yoshina-Ishii, C.; Jaroniec, M.; Ozin, G. A. Synthesis and Properties of 1,3,5-Benzene Periodic Mesoporous Organosilica (PMO): Novel Aromatic PMO with Three Point Attachments and Unique Thermal Transformations. *J. Am. Chem. Soc.* **2002**, *124*, 13886–13895.

(50) Nakajima, K.; Lu, D.; Kondo, J. N.; Tomita, I.; Inagaki, S.; Hara, M.; Hayashi, S.; Domen, K. Synthesis of highly ordered hybrid mesoporous material containing ethenylene (–CH=CH–) within the silicate framework. *Chem. Lett.* **2003**, *32*, 950–951.

(51) Asefa, T.; Kruk, M.; MacLachlan, M. J.; Coombs, N.; Grondy, H.; Jaroniec, M.; Ozin, G. A. Novel Bifunctional Periodic Mesoporous Organosilicas, BPMOs: Synthesis, Characterization, Properties and in-Situ Selective Hydroboration-Alcoholysis Reactions of Functional Groups. *J. Am. Chem. Soc.* **2001**, *123*, 8520–8530.

(52) Yang, Y.; Sayari, A. Molecularly Ordered Biphenyl-Bridged Mesoporous Organosilica Prepared under Acidic Conditions. *Chem. Mater.* **2007**, *19*, 4117–4119.

(53) Fan, J.; Yu, C.; Lei, J.; Zhang, Q.; Li, T.; Tu, B.; Zhou, W.; Zhao, D. Low-Temperature Strategy to Synthesize Highly Ordered Mesoporous Silicas with Very Large Pores. *J. Am. Chem. Soc.* **2005**, *127*, 10794–10795.

(54) Kruk, M.; Hui, C. M. Synthesis and Characterization of Large-pore FDU-12 Silica. *Microporous Mesoporous Mater.* **2008**, *114*, 64–73.

(55) Hartono, B. S.; Qiao, S. Z.; Jack, K.; Ladewig, B. P.; Hao, Z.; Lu, G. Q. M. Improving Adsorbent Properties of Cage-like Ordered Amine Functionalized Mesoporous Silica with Very Large Pores for Bioadsorption. *Langmuir* **2009**, *25*, 6413–6424.

(56) Huang, L.; Yan, X.; Kruk, M. Synthesis of Ultra-large-pore FDU-12 Silica with Face-centered Cubic Structure. *Langmuir* **2010**, *26*, 14871–14878.

(57) Mandal, M.; Kruk, M. Versatile Approach to Synthesis of 2-D Hexagonal Ultra-Large-Pore Periodic Mesoporous Organosilicas. *J. Mater. Chem.* **2010**, *20*, 7506–7516.

(58) Sing, K. S. W.; Everett, D. H.; Haul, R. A. W.; Moscou, L.; Pierotti, R. A.; Rouquerol, J.; Siemieniowska, T. Reporting physisorption data for gas/solid systems with special reference to the determination of surface area and porosity (Recommendations 1984). *Pure Appl. Chem.* **1985**, *57*, 603–619.

(59) Jaroniec, M.; Kruk, M.; Olivier, J. P. Standard Nitrogen Adsorption Data for Characterization of Nanoporous Silicas. *Langmuir* **1999**, *15*, 5410–5413.

(60) Barrett, E. P.; Joyner, L. G.; Halenda, P. P. The determination of pore volume and area distributions in porous substances. I.

Computations from nitrogen isotherms. *J. Am. Chem. Soc.* **1951**, *73*, 373–380.

(61) Kruk, M.; Jaroniec, M.; Sayari, A. Application of Large Pore MCM-41 Molecular Sieves To Improve Pore Size Analysis Using Nitrogen Adsorption Measurements. *Langmuir* **1997**, *13*, 6267–6273.

(62) Matos, J. R.; Kruk, M.; Mercuri, L. P.; Jaroniec, M.; Zhao, L.; Kamiyama, T.; Terasaki, O.; Pinnavaia, T. J.; Liu, Y. Ordered Mesoporous Silica with Large Cage-Like Pores: Structural Identification and Pore Connectivity Design by Controlling the Synthesis Temperature and Time. *J. Am. Chem. Soc.* **2003**, *125*, 821–829.

(63) Ravikovitch, P. I.; Neimark, A. V. Density functional theory of adsorption in spherical cavities and pore size characterization of templated nanoporous silicas with cubic and three-dimensional hexagonal structures. *Langmuir* **2002**, *18*, 1550–1560.

(64) Cerveau, G.; Corriu, R. J. P.; Framery, E. Sol-gel process: influence of the temperature on the textural properties of organosilsesquioxane materials. *J. Mater. Chem.* **2000**, *10*, 1617–1622.

(65) Vercaemst, C.; Jones, J. T. A.; Khimyak, Y. Z.; Martins, J. C.; Verpoort, F.; Van Der Voort, P. Spectroscopic evidence of thermally induced metamorphosis in ethylene-bridged periodic mesoporous organosilicas. *Phys. Chem. Chem. Phys.* **2008**, *10*, 5349–5352.

(66) Asefa, T.; MacLachlan, M. J.; Grondy, H.; Coombs, N.; Ozin, G. A. Metamorphic channels in periodic mesoporous methylenesilica. *Angew. Chem., Int. Ed.* **2000**, *39*, 1808–1811.

(67) Asefa, T.; Kruk, M.; Coombs, N.; Grondy, H.; MacLachlan, M. J.; Jaroniec, M.; Ozin, G. A. Novel Route to Periodic Mesoporous Aminosilicas, PMAs: Ammonolysis of Periodic Mesoporous Organosilicas. *J. Am. Chem. Soc.* **2003**, *125*, 11662–11673.

(68) Kim, T. W.; Ryoo, R.; Kruk, M.; Gierszal, K. P.; Jaroniec, M.; Kamiya, S.; Terasaki, O. Tailoring the pore structure of SBA-16 silica molecular sieve through the use of copolymer blends and control of synthesis temperature and time. *J. Phys. Chem. B* **2004**, *108*, 11480–11489.

(69) Kruk, M.; Jaroniec, M. Argon Adsorption at 77 K as a Useful Tool for the Elucidation of Pore Connectivity in Ordered Materials with Large Cagelike Mesopores. *Chem. Mater.* **2003**, *15*, 2942–2949.

(70) Kleitz, F.; Liu, D.; Anilkumar, G. M.; Park, I.-S.; Solovyov, L. A.; Shmakov, A. N.; Ryoo, R. Large Cage Face-Centered-Cubic Fm3m Mesoporous Silica: Synthesis and Structure. *J. Phys. Chem. B* **2003**, *107*, 14296–14300.

(71) Fan, J.; Yu, C.; Gao, F.; Lei, J.; Tian, B.; Wang, L.; Luo, Q.; Tu, B.; Zhou, W.; Zhao, D. Cubic mesoporous silica with large controllable entrance sizes and advanced adsorption properties. *Angew. Chem., Int. Ed.* **2003**, *42*, 3146–3150.

(72) Liu, J.; Bai, S.; Zhong, H.; Li, C.; Yang, Q. Tunable Assembly of Organosilica Hollow Nanospheres. *J. Phys. Chem. C* **2010**, *114*, 953–961.

(73) Tan, H.; Liu, N. S.; He, B.; Wong, S. Y.; Chen, Z.-K.; Li, X.; Wang, J. Facile synthesis of hybrid silica nanocapsules by interfacial templating condensation and their application in fluorescence imaging. *Chem. Commun.* **2009**, 6240–6242.

(74) Huo, Q.; Liu, J.; Wang, L.-Q.; Jiang, Y.; Lambert, T. N.; Fang, E. A New Class of Silica Cross-Linked Micellar Core-Shell Nanoparticles. *J. Am. Chem. Soc.* **2006**, *128*, 6447–6453.

(75) Hamley, I. W.; Daniel, C.; Mingvanish, W.; Mai, S.-M.; Booth, C.; Messe, L.; Ryan, A. J. From Hard Spheres to Soft Spheres: The Effect of Copolymer Composition on the Structure of Micellar Cubic Phases Formed by Diblock Copolymers in Aqueous Solution. *Langmuir* **2000**, *16*, 2508–2514.

(76) Morishige, K.; Tateishi, M.; Hirose, F.; Aramaki, K. Change in Desorption Mechanism from Pore Blocking to Cavitation with Temperature for Nitrogen in Ordered Silica with Cagelike Pores. *Langmuir* **2006**, *22*, 9220–9224.